

Two-impurity Kondo effect in double-quantum-dot systems: Effect of interdot kinetic exchange coupling

著者	泉田 渉
journal or publication title	Physical review. B
volume	62
number	15
page range	10260-10267
year	2000
URL	http://hdl.handle.net/10097/35716

doi: 10.1103/PhysRevB.62.10260

Two-impurity Kondo effect in double-quantum-dot systems: Effect of interdot kinetic exchange coupling

Wataru Izumida*

*Department of Applied Physics, Hokkaido University, Sapporo 060-8628, Japan
and Tarucha Mesoscopic Correlation Project, ERATO, JST, NTT Atsugi Research and Development Center, Atsugi-shi,
Kanagawa 243-0198, Japan*

Osamu Sakai

*Department of Physics, Tokyo Metropolitan University, Tokyo 192-0397, Japan
(Received 7 December 1999)*

Tunneling conductance through two quantum dots, which are connected in series to left and right leads, is calculated by using the numerical renormalization group method. As the hopping between the dots increases from a very small value, the following states continuously appear: (i) Kondo singlet state of each dot with its adjacent-site lead, (ii) singlet state between the local spins on the dots, and (iii) double occupancy in the bonding orbital of the two dots. The conductance shows peaks at the crossover regions between these states. The peak at the boundary between (i) and (ii) especially has the unitarity limit value of $2e^2/h$ because of coherent connection through the lead-dot-dot-lead. For the strongly correlated cases, the characteristic energy scale of the coherent peak shows anomalous decrease relating to the quantum critical transition known for the two-impurity Kondo effect. The two dot systems give a new realization of the two-impurity Kondo problem.

I. INTRODUCTION

Dilute magnetic impurities in metal give rise to the single-impurity Kondo effect.^{1,2} The antiferromagnetic coupling between spins on impurities J , such as the Ruderman-Kittel-Kasuya-Yosida interaction, would compete with the Kondo effect. To study such competition effect, the two impurities in metal have been studied extensively.³⁻¹⁴ If the Kondo binding energy is much larger than J ($T_K \gg J$), each local spin on the magnetic impurity forms the Kondo singlet state with the conduction electrons. On the other hand for $T_K \ll J$, the two local spins form the local spin singlet state. From the numerical renormalization group (NRG) calculation, Jones *et al.* pointed out that the transition between the two states occurs as a quantum critical phenomenon.⁴ However, it was pointed out⁸ that the critical transition was associated with the extra symmetry between the even and odd channels implicitly assumed in the work of Jones *et al.* In general there is an asymmetry between the two channels, caused by the parity splitting terms such as the d - d hopping term between the impurity atoms. Under the asymmetry, only a crossover occurs rather than the critical transition. Theoretical refinement has been done on this problem.^{13,14}

It might be difficult to observe the two-impurity effect in metal systems as pointed out by previous studies, because the alloy contains many types of impurity pairs, and the coupling between impurities is fixed in each material. Recently, the Kondo effect was observed in single quantum dot systems.¹⁵⁻¹⁹ The experimental data show good agreement with the results of numerical calculations based on the single-impurity Anderson model.²⁰ These works demonstrated that the quantum dot systems are suitable for sensitive experiment of the Kondo problem. On the double-quantum-dot (DQD) systems, each dot corresponds to an impurity

atom, and the coupling between the dots, the d - d hopping term, can be changed freely by applying the split gate voltage between the dots.²¹ It would be expected that we can investigate the two-impurity effect systematically in the DQD systems.

For the DQD systems, in which the two dots are connected to the left lead and the right lead in a series as "lead-dot-dot-lead," there are several theoretical works including the Kondo effect.²²⁻²⁸ We have reported the large enhancement of the tunneling conductance through the two dots when the condition $J_{LR}^{\text{eff}} \sim T_K^0$ holds, by using the NRG calculation.²⁵ Here $J_{LR}^{\text{eff}} = 4t^2/U$ is the antiferromagnetic kinetic exchange coupling between the two dots, t is the hopping between the two dots, U is the Coulomb repulsion on the dot, and T_K^0 is the Kondo temperature at $t=0$. We note that the antiferromagnetic coupling is the inevitable effect due to the kinetic process t and the Coulomb repulsion on the dot U . There are investigations with the slave boson mean field theory (SBMFT). Aono *et al.* had already studied the same model as us, however they could not find the relation $J_{LR}^{\text{eff}} \sim T_K^0$ on the peak of the conductance pointed out by us because the SBMFT cannot treat the kinetic exchange process properly.²⁴ Georges and Meir introduced the antiferromagnetic coupling J between the two dots by artifice in the model, and discussed the effect related to the critical transition on the conductance by using the SBMFT.²⁶ However the introduction of the artificial J in the model and the calculation of the conductance within the SBMFT framework raise the following questions: (a) Does the effect of antiferromagnetic coupling pointed by Georges and Meir actually appear in the DQD systems, since the hopping itself breaks the quantum critical transition?^{8,9} (b) If it appears, however, how do the conflicting effects of t , the kinetic exchange coupling

that would cause the critical transition and the parity splitting that suppress the critical transition, compete? (c) How do they appear in the conductance? Since the SBMFT could not treat the kinetic exchange process properly, this approximation for the two-impurity Kondo problem like the DQD systems seems to be unfavorable. A reliable calculation is necessary for such a sensitive problem.

In this paper, we present a detailed investigation of the Kondo effect in the DQD systems, paying special attention to the roles of the d - d hopping term. The numerical calculation is performed by using the NRG method. This numerical method is known to be a reliable one for the two-impurity Kondo problem.^{3-6,8,9,14} We calculate the tunneling conductance through the two dots. We note that some preliminary results were presented at SCES98,²⁵ and one of the central results was presented at LT22.²⁸

We find that the following states continuously appear when the hopping between the two dots increases from a very small value: (i) Kondo singlet state ($t \ll U$, $J_{LR}^{\text{eff}} \ll T_K^0$), (ii) singlet state between local spins on the dots ($t \ll U$, $J_{LR}^{\text{eff}} \gg T_K^0$), and (iii) double occupancy in the bonding orbital of the two dots ($t \geq U$). The conductance shows peaks at the crossover regions between these states. The ‘main peak’ at the boundary between (i) and (ii) with the condition $J_{LR}^{\text{eff}} \sim T_K^0$ has the unitarity limit value of $2e^2/h$ because of coherent connections through the lead-dot-dot-lead. Especially for the strongly correlated cases, the width of the main peak becomes very narrow and the characteristic temperature of the peak is largely suppressed compared with the Kondo temperature of the single dot systems T_K^0 . These anomalies of the main peak closely relate to the quantum critical phenomenon in the two-impurity Kondo problem. The quantitative calculation in this paper gives new realization to the two-impurity Kondo problem, and suggests the possibility of a systematic study of the anomalous two-impurity Kondo effect in the DQD systems.

The formulation is presented in Sec. II. The numerical results are presented in Sec. III. The summary and discussion are given in Sec. IV.

II. FORMULATION

We investigate the following Hamiltonian for the DQD systems where the two dots are connected to the left lead and the right lead in a series:

$$H = H_1 + H_d + H_{1-d}, \quad (1)$$

$$H_1 = \sum_{k\sigma} \varepsilon_k c_{Lk\sigma}^\dagger c_{Lk\sigma} + \sum_{q\sigma} \varepsilon_q c_{Rq\sigma}^\dagger c_{Rq\sigma}, \quad (2)$$

$$H_d = \varepsilon_{d,L} \sum_{\sigma} n_{d,L\sigma} + \varepsilon_{d,R} \sum_{\sigma} n_{d,R\sigma} + \left(-t \sum_{\sigma} d_{L\sigma}^\dagger d_{R\sigma} + \text{H.c.} \right) + U_L n_{d,L\uparrow} n_{d,L\downarrow} + U_R n_{d,R\uparrow} n_{d,R\downarrow}, \quad (3)$$

$$H_{1-d} = \sum_{k\sigma} V_{Lk} d_{L\sigma}^\dagger c_{Lk\sigma} + \sum_{q\sigma} V_{Rq} d_{R\sigma}^\dagger c_{Rq\sigma} + \text{H.c.} \quad (4)$$

H_1 is the Hamiltonian for the electrons in the left and right leads. H_d is that in the left and right dots. H_{1-d} is that for the

tunneling between the left lead and the left dot, and between the right lead and the right dot. The suffices L, R mean the left and the right, respectively. $c_{Lk\sigma}$ is the annihilation operator of the electron in the left lead, $d_{L\sigma}$ is that in the left dot. $n_{d,L\sigma} = d_{L\sigma}^\dagger d_{L\sigma}$ is the number operator of the left dot. ε_k is the energy of the state k in the left lead. $\varepsilon_{d,L}$ is the energy of the orbital in the left dot. The quantity t is the matrix element between the left and right dots, and we refer to it as the ‘hopping’ between the dots hereafter. U_L is the Coulomb interaction between the electrons in the left dot. V_L is the matrix element between the left dot and the left lead.

Here we consider only the single orbital in each of the dots. This situation is justified when the typical energy splitting between the orbitals in the dot is larger than the typical broadening of the energy levels $\delta\varepsilon_d \gg \Delta$, and when the temperature is smaller than the typical Coulomb repulsion between the electrons in the dots $T \ll U$.^{20,29} (The Kondo effect is not important in the case of $T \geq U$.) We consider only the on-site Coulomb interaction between the electrons. Furthermore, we consider only the nearest neighboring tunneling, between the dot and its adjacent-site lead, between the two dots. The energies $\varepsilon_{d,L}$ and $\varepsilon_{d,R}$ can be changed by applying the gate voltage on the dots. V_{Lk} (V_{Rq}) can also be changed by applying the split gate voltage between the left (right) dot and the left (right) lead. t can be changed by applying the split gate voltage between the left dot and the right dot.

In this paper we consider only the symmetric case with respect to the exchange of the left and the right. This situation is written with the following relations; $\varepsilon_d \equiv \varepsilon_{d,L} = \varepsilon_{d,R}$, $U \equiv U_L = U_R$, and $\Delta \equiv \Delta_L = \Delta_R = \pi |V|^2 \rho_c$. (Δ is the hybridization strength between the dots and the leads, $V \equiv V_{Lk} = V_{Rk}$, ρ_c is the density of states in the leads. Here we consider that there is no k dependence in the matrix element and the density of states.³⁰) The model can be mapped into the two-channel Anderson Hamiltonian by the unitary transform for the operators of the dots and the operators of the leads.²⁵ Furthermore we consider the situation where there is one electron in each dot by adjusting the gate voltage on the dot, $\langle n_{d,L} \rangle = 1$, $\langle n_{d,R} \rangle = 1$.

We solve the Hamiltonian by using the NRG method, and calculate the conductance from the current correlation function within the linear response theory.^{25,29,31} (For detailed calculation of the conductance, see appendix of Ref. 31.)

At zero temperature, the conductance can be rewritten by using the effective parameters of the fixed point noninteracting Anderson Hamiltonian as follows:

$$G = \frac{2e^2}{h} |\Delta \mathcal{G}_e(0^+) - \Delta \mathcal{G}_o(0^+)|^2 = \frac{2e^2}{h} \frac{4(t^{\text{eff}}/\Delta^{\text{eff}})^2}{[1 + (t^{\text{eff}}/\Delta^{\text{eff}})^2]^2}. \quad (5)$$

We have used the relation, $\mathcal{G}_p = z_p / (\omega - \varepsilon_p^{\text{eff}} + i\Delta_p^{\text{eff}})$, $z_p = \Delta_p^{\text{eff}}/\Delta$, ($p = e, o$), at $T = 0$. Here the suffix p denotes the even and odd parity orbitals in the two dots. We note that the even orbital is the bonding orbital, and the odd orbital is the antibonding orbital. We now consider the case of $\langle n_e \rangle + \langle n_o \rangle = 2$, then $t^{\text{eff}} \equiv -\varepsilon_e^{\text{eff}} = \varepsilon_o^{\text{eff}} \geq 0$, $\Delta^{\text{eff}} \equiv \Delta_e^{\text{eff}} = \Delta_o^{\text{eff}}$. Here t^{eff} is the effective hopping between the dots, and Δ^{eff} is the effective hybridization strength between the leads and the dots. At $T = 0$, we calculate the effective parameters from the

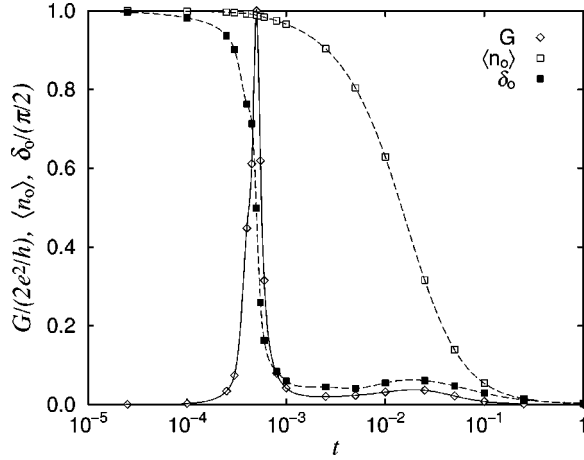


FIG. 1. Conductance G , occupation number in the odd orbital of the two dots $\langle n_o \rangle$, and phase shift of the odd channel δ_o , as a function of the hopping t at $T=0$. We note the relations between the even and odd orbitals, $\langle n_e \rangle = 2 - \langle n_o \rangle$, $\delta_e = \pi - \delta_o$. $\Delta/\pi U = 1.5 \times 10^{-2}$.

analysis of the flow chart of the renormalized energy level structure in the NRG calculation, and then calculate the conductance from Eq. (5).

III. NUMERICAL RESULTS

In numerical calculation we choose half of the bandwidth as an energy unit. The Coulomb repulsion is fixed at $U = 0.1$ throughout this paper. We calculate the conductance as a function of the hopping t for various hybridization strengths Δ . (As noted previously, t and Δ can be changed by applying the split gate voltage between the dots and between the dots and the leads, respectively.) When the gate voltage on the dots is fixed at $\varepsilon_d = -U/2$, then the DQD is in the half-filled case, i.e., each dot contains one electron.

In Secs. III A and III B we present the numerical results at zero temperature $T=0$, and in Sec. III C we present the results at finite temperatures.

A. Conductance in the strongly correlated case

First we present the conductance in the strongly correlated case with the hybridization strength satisfying $\Delta/\pi = 1.5 \times 10^{-3}$ ($\Delta/\pi U = 1.5 \times 10^{-2}$, i.e., $u \equiv U/\pi\Delta \approx 6.8$).

We show the conductance at $T=0$ as a function of the hopping t in Fig. 1. (The occupation number and the phase shift are also shown in Fig. 1.) There are two peaks in the conductance, the large peak near $t \sim 5 \times 10^{-4}$, and the small peak near $t \sim 2 \times 10^{-2}$. (Hereafter we call the large peak the ‘‘main peak.’’) Why do these peaks appear? In later paragraphs we will analyze various quantities for the parameter cases showing the peaks.

The density of states on the even orbital of the two dots $\rho_e(\omega)$ for several t cases is shown in Fig. 2. [The relation $\rho_e(\omega) = \rho_o(-\omega)$ holds for $\langle n_e \rangle + \langle n_o \rangle = 2$, where $\rho_o(\omega)$ is the density of states on the odd orbital of the two dots.] At $t=0$, there is the Kondo peak on the Fermi energy. (Fermi energy corresponds to $\omega=0$.) Naturally, this Kondo peak is caused by the Kondo singlet states between the left lead and the left dot, and between the right lead and the right dot. As

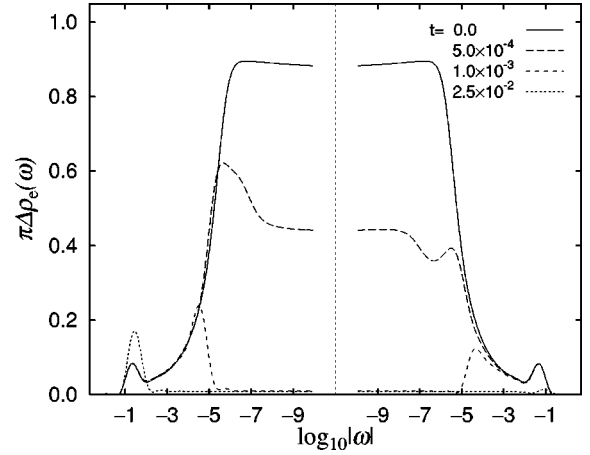


FIG. 2. Density of states on the even orbital of the two dots, $\rho_e(\omega)$. We note the relation $\rho_o(\omega) = \rho_e(-\omega)$, where $\rho_o(\omega)$ is the density of states on the odd orbital. $\Delta/\pi U = 1.5 \times 10^{-2}$.

t increases to $t = 5 \times 10^{-4}$, the conductance has the main peak and the strength of $\rho_e(\omega \sim 0)$ becomes half of that at $t=0$. In this region we can consider that the Kondo effect with the spins on the orbitals extending the two dots, the even and the odd orbitals, occurs. As t increases more, the conductance decreases rapidly, and the strength of $\rho_e(\omega \sim 0)$ is largely suppressed as shown at $t = 1.0 \times 10^{-3}$. This suppression means the disappearance of the Kondo coupling between the leads and the dots. t becomes even larger, the conductance has the small peak at $t \sim 2 \times 10^{-2}$. At $t = 2.5 \times 10^{-2}$, the density of states on the even and odd orbitals have peaks at $\mp \omega \sim 10^{-1}$, respectively, from Fig. 2. At the same time the occupation numbers begin to change as shown in Fig. 1. ($\langle n_e \rangle \approx 1.5$, $\langle n_o \rangle \approx 0.5$ at $t \approx 1.5 \times 10^{-2}$.)

Here we note the following two points: First, the condition $J_{LR}^{\text{eff}} \sim T_K^0$ holds at $t \approx 5 \times 10^{-4}$, where $J_{LR}^{\text{eff}} \equiv 4t^2/U$. ($T_K^0 = 3.78 \times 10^{-6}$ is the Kondo temperature at $t=0$, with the expression $T_K^0 = \sqrt{U\Delta/2} \exp[-\pi U/8\Delta + \Delta/2U]$,¹ then $J_{LR}^{\text{eff}}/T_K^0 \approx 2.65$ at $t = 5.0 \times 10^{-4}$.) Second, as seen from Fig. 1, the occupation numbers of the even and the odd orbitals for $t \lesssim 1.0 \times 10^{-3}$ are almost equal to each other, $\langle n_e \rangle \approx \langle n_o \rangle \approx 1$. For $t \gtrsim 1.0 \times 10^{-1}$, the two electrons occupy the even orbital. The border between them is at $t \sim U/4 (= 2.5 \times 10^{-2})$.

The above analysis implies the following scenario. In the case of $t \ll U/4 (= 2.5 \times 10^{-2})$, the hopping t causes the anti-ferromagnetic kinetic exchange coupling J_{LR}^{eff} . For smaller hopping cases with $J_{LR}^{\text{eff}} \ll T_K^0$, there are Kondo singlet states between the left lead and the left dot, and between the right lead and the right dot. As t increases and $J_{LR}^{\text{eff}} \gtrsim T_K^0$, the two local spins on each dot form the local singlet state. At the crossover region between two states we have a main peak with the unitarity limit value of $2e^2/h$ in the conductance. This will indicate that the leads and the dots are coherently connected by the even and the odd orbital states. When t becomes even larger and the condition $t \gtrsim U/4$ holds, the local spins do not appear; instead, the two electrons occupy the even orbital. The small peak of the conductance reflects the change of the electronic states in the DQD.

Here we show the effective parameters t^{eff} and Δ^{eff} as a function of t in Fig. 3. (We note that the effective parameters

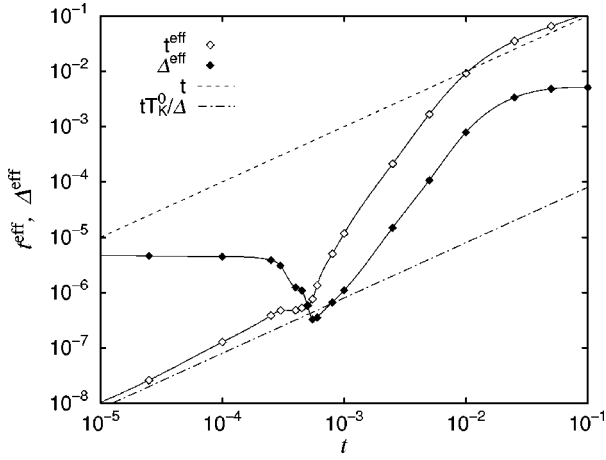


FIG. 3. Effective parameters t^{eff} , Δ^{eff} of the fixed point noninteracting Anderson Hamiltonian, given by the analysis of the flow chart of the renormalized energy level structure in the NRG calculation. $\Delta/\pi U = 1.5 \times 10^{-2}$.

have been used already for the calculation of the conductance shown in Fig. 1.) In the $t \leq 10^{-4}$ case, the effective parameters behave as $t^{\text{eff}} \sim tT_K^0/\Delta$, $\Delta^{\text{eff}} \sim T_K^0$. Then the conductance coincides with the noninteracting one when one substitutes the effective parameters into Eq. (5). As t increases to $t \sim 5 \times 10^{-4}$, Δ^{eff} decreases once, and it has local minimum, and then it increases. At the same time the slope of t^{eff} decreases once and then increases. When t^{eff} and Δ^{eff} coincide with each other, the conductance has a peak at $t \sim 5 \times 10^{-4}$, i.e., $J_{\text{LR}}^{\text{eff}} \sim T_K^0$. As t increases slightly beyond this point, the conductance sharply decreases because Δ^{eff} decreases to the minimum even though t^{eff} increases. Here we stress that the relation $t^{\text{eff}} \sim \Delta^{\text{eff}}$ holds when $J_{\text{LR}}^{\text{eff}} \sim T_K^0$, and at the same time Δ^{eff} becomes very small.⁹ In this meaning, the crossover seems to be characterized by the relation $t^{\text{eff}} \sim \Delta^{\text{eff}}$. This relation gives the unitarity peak of the tunneling conductance as seen from Eq. (5). When t increases further, the ratio $t^{\text{eff}}/\Delta^{\text{eff}}$ increases gradually in the region $t \leq U/4$ ($= 2.5 \times 10^{-2}$). At $t \sim U/4$, the ratio $t^{\text{eff}}/\Delta^{\text{eff}}$ begins to decrease and then increases. Therefore the conductance shows a broad peak near the region $t \sim U/4$. For the $t \geq U/4$ case, the effective parameters behave as $t^{\text{eff}} \sim t$, $\Delta^{\text{eff}} \sim \Delta$. We note that the conductance has the expression of the noninteracting one itself in the $t \geq U/4$ region.

Finally we compare the phase shift and the occupation number shown in Fig. 1. The phase shift of the odd orbital δ_o rapidly changes from $\pi/2$ to 0 near $t \sim 5 \times 10^{-4}$, even though $\langle n_o \rangle$ still remains at $\langle n_o \rangle \sim 1$. Friedel's sum rule in each channel does not hold, as pointed out previously.⁹ It seems that this behavior is enhanced when the antiferromagnetic coupling between the two sites competes with the Kondo effect.

B. From weakly to strongly correlated cases

In this subsection we present the numerical results of the conductance for various $\Delta/\pi U$ cases within $1.5 \times 10^{-2} \leq \Delta/\pi U \leq 6.0 \times 10^{-2}$. ($1.7 \leq u \leq 6.8$. The hybridization strength is changed in $1.5 \times 10^{-3} \leq \Delta/\pi \leq 6.0 \times 10^{-3}$, and the Coulomb repulsion is fixed at $U = 0.1$.) We confirm the sce-

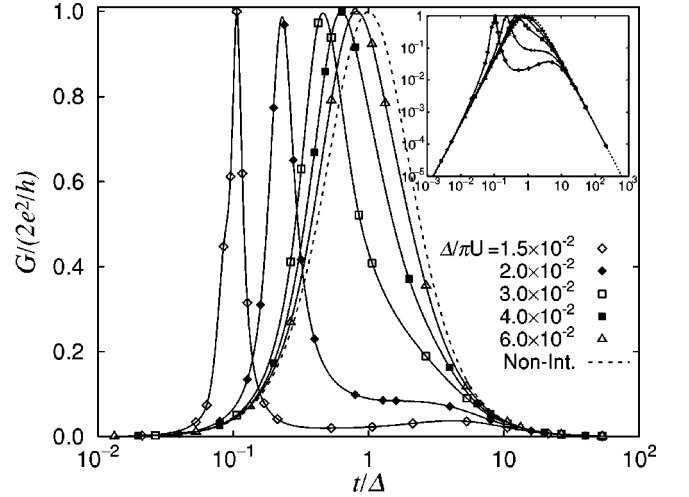


FIG. 4. Conductance as a function of t at zero temperature, from the weakly to strongly correlated cases in $1.5 \times 10^{-2} \leq \Delta/\pi U \leq 6.0 \times 10^{-2}$. The broken line shows the conductance for the noninteracting ($U=0$) case.

nario shown in the previous subsection that $t^{\text{eff}} \sim \Delta^{\text{eff}}$ holds at the main peak of the conductance with $J_{\text{LR}}^{\text{eff}} \sim T_K^0$. We also demonstrate how the kinetic exchange process appears in the conductance for arbitrary $\Delta/\pi U$ cases.

The calculated conductance is shown in Fig. 4. The horizontal axis is the hopping normalized by the hybridization strength, t/Δ . From inset of Fig. 4, the conductance almost overlaps on the noninteracting curve in the regions $t \ll \Delta$ and $t \gg \Delta$. These regions should be classified $J_{\text{LR}}^{\text{eff}} \leq T_K^0$ and $t \gg U/4$, respectively, from the analysis in the previous subsection. The conductance is very small in these regions, however these uniform properties should be useful in arranging the experimental data under uncertain U/Δ cases.

All curves have a main peak with strength $2e^2/h$. For weakly correlated cases of $\Delta/\pi U \geq 4 \times 10^{-2}$, the conductance almost coincides with the noninteracting one throughout the t region. As U/Δ increases, the main peak shifts to the small t/Δ side, and the peak width becomes narrower.

We have already found the relation $J_{\text{LR}}^{\text{eff}} \sim T_K^0$ at the main peak position for the $\Delta/\pi U = 1.5 \times 10^{-2}$ case in Sec. III A. Here we show the ratio $J_{\text{LR}}^{\text{eff}}/T_K^0$ at the main peak position for various $\Delta/\pi U$ cases in Table I. We can see the relation $J_{\text{LR}}^{\text{eff}} \sim T_K^0$ commonly.²⁵ [The relation at the main peak $J_{\text{LR}}^{\text{eff}} \sim T_K^0$ would be generalized to $E_B \sim T_K^0$ for the weakly correlated cases, where $E_B = \sqrt{(2t)^2 + (U/2)^2} - U/2$ is the singlet binding energy between the two dots.]

From the analysis in the previous and present subsection we can conclude the following effect of the hopping term. For the small t case with $J_{\text{LR}}^{\text{eff}} \leq T_K^0$ (i), the Kondo singlet state is formed on the left (right) dot with its adjacent-site lead.

TABLE I. Ratios $J_{\text{LR}}^{\text{eff}}/T_K^0$ and E_B/T_K^0 at the main peak position of the conductance.

$\Delta/\pi U$	1.5×10^{-2}	2×10^{-2}	3×10^{-2}	4×10^{-2}	6×10^{-2}
$J_{\text{LR}}^{\text{eff}}/T_K^0$	2.66	2.34	2.15	2.09	2.23
E_B/T_K^0	2.66	2.34	2.14	2.04	2.05

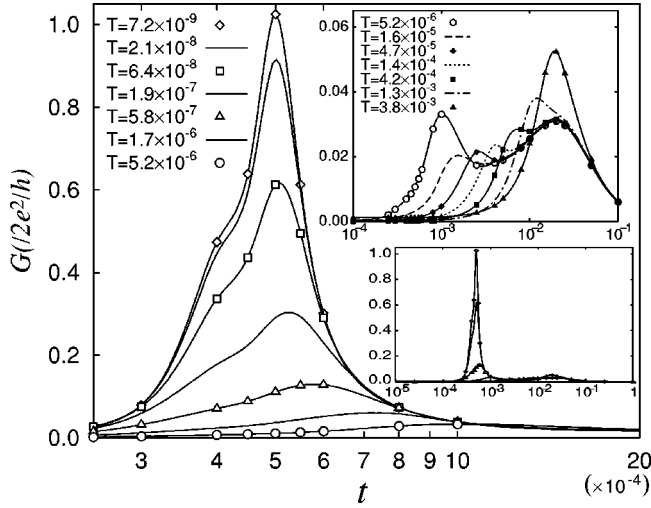


FIG. 5. Temperature dependence of the conductance. Main figure is the temperature dependence near the main peak at $t \sim 5 \times 10^{-4}$. Inset figure at the upper right is the temperature dependence near the small peak at $t \sim 2.5 \times 10^{-2}$. Inset figure at the lower right is the conductance in all over t . $\Delta/\pi U = 1.5 \times 10^{-2}$.

On the other hand, for the large t case with $J_{LR}^{\text{eff}} \gg T_K^0$ (ii), the local spins on each of the dots couple as the singlet state. In the intermediate region, the Kondo effect of the local spins on the orbitals extending on the two dots (i.e., even and odd orbitals) occurs. The main peak of the conductance appears around the boundary between (i) and (ii) reflecting the coherent connection of the leads and the dots. As U/Δ increases, the Kondo temperature T_K^0 exponentially decreases, the condition $J_{LR}^{\text{eff}} \sim T_K^0$ holds at the smaller t/Δ , then the main peak shifts to the smaller t/Δ side. At the same time, the width of the peak becomes extremely narrow compared with the decreasing T_K^0 . This fact has been already shown as the steep minimum of Δ^{eff} in Fig. 3. We note that this narrowing is closely related to the quantum critical transition between the Kondo singlet state and the local singlet state in the two-impurity Kondo model.⁴ The shifting and narrowing behaviors shown here are also pointed out with the SBMFT with artificial addition to the model of the antiferromagnetic

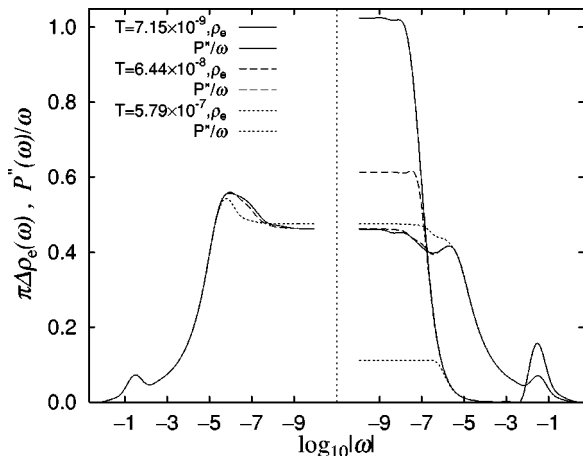


FIG. 6. Density of states $\rho_e(\omega)$ and current spectrum $P''(\omega)/\omega$ at $t = 5.0 \times 10^{-4}$ for finite temperatures. (The spectrum, which has only the positive region $\omega \geq 0$, is the current spectrum.)

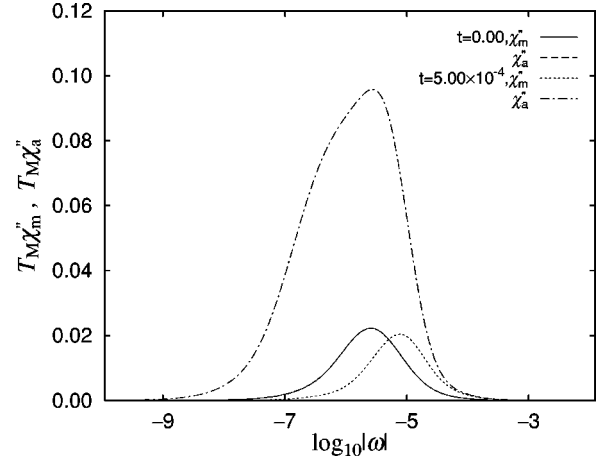


FIG. 7. Two sorts of the magnetic excitation spectra $\chi_m''(\omega)$ and $\chi_a''(\omega)$ at $T=0$. We note that the two spectra agree with each other at $t=0$.

coupling between dots.²⁶ However, the SBMFT calculation should be checked by the method treating the kinetic exchange term properly. As noted in the introduction, the hopping term causes two conflicting effects on the critical transition of the two-impurity systems. One is the kinetic exchange coupling J_{LR}^{eff} , which causes the ‘‘critical’’ transition through the competition with the Kondo effect. Another is the parity splitting, which suppresses the critical transition. To the best of our knowledge, the calculation in this section is the first reliable quantitative result of the two-impurity Kondo problem in the DQD systems.

There is also another small peak (or shoulder) structure for the strongly correlated cases of $\Delta/\pi U \lesssim 2 \times 10^{-2}$ ($u \gtrsim 5$) at the larger t side of the main peak. In the previous subsection, we found that the small peak appears around the boundary between (ii) and (iii). However for the weakly correlated cases, the small peak could not be recognized because the condition of the border (i)-(ii) and (ii)-(iii) could not be distinguished clearly.

C. Temperature dependence of the conductance

In this subsection we present the conductance in finite temperature. We calculate the conductance at finite temperatures by using the following formula:³¹

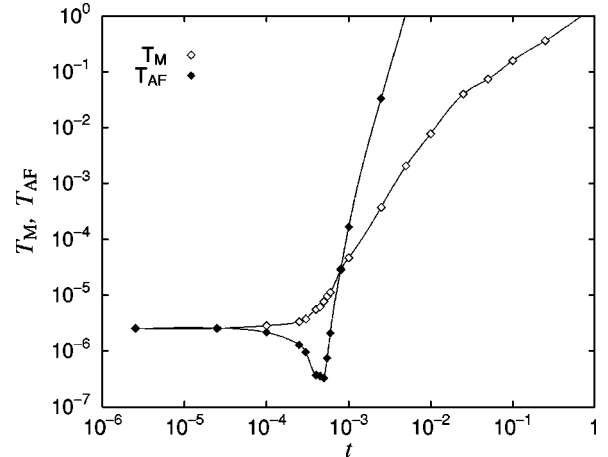


FIG. 8. Two characteristic energies T_M and T_{AF} .

TABLE II. Characteristic energies at the main peak position.

$\Delta/\pi U$	1.5×10^{-2}	2×10^{-2}	3×10^{-2}	4×10^{-2}	6×10^{-2}
T_{AF}	3.28×10^{-7}	9.77×10^{-6}	3.97×10^{-4}	1.50×10^2	3.01×10^2
T_M	7.66×10^{-6}	5.64×10^{-5}	7.73×10^{-4}	3.47×10^{-3}	1.20×10^{-2}
$T_{M,0}$	2.55×10^{-6}	2.47×10^{-5}	2.31×10^{-4}	8.02×10^{-4}	3.22×10^{-3}

$$G = \frac{2e^2}{h} \lim_{\omega \rightarrow 0} \frac{P''(\omega)}{\omega}. \quad (6)$$

Here $P''(\omega)$ is the ‘‘current spectrum’’ for the current operator $J \equiv \dot{N}_L - \dot{N}_R$ written as follows:

$$P''(\omega) = \frac{\pi^2 \hbar^2}{4} \frac{1}{Z} \sum_{n,m} (e^{-\beta E_m} - e^{-\beta E_n}) |\langle n | J | m \rangle|^2 \times \delta[\omega - (E_n - E_m)], \quad (7)$$

where \dot{N}_L is the time differentiation of the electron number in the left lead, $Z = \sum_n e^{-\beta E_n}$ is the partition function of the system, and β is the inverse of the temperature ($\beta = 1/T$).

First we show the conductance at various temperatures for the $\Delta/\pi U = 1.5 \times 10^{-2}$ case in Fig. 5. As the temperature increases from $T \sim 10^{-8}$, the height of the main peak gradually decreases. At the same time the peak position shifts to the larger t . We note that $T \sim 10^{-8}$ is much lower than T_K^0 ($T_K^0 = 3.78 \times 10^{-6}$).

To discuss the characteristic behaviors of the conductance in finite temperature, we show the density of states $\rho_e(\omega)$ and the current spectrum (divided by ω) $P''(\omega)/\omega$ at $t = 5.0 \times 10^{-4}$ in Fig. 6. As the temperature increases to $T = 6.44 \times 10^{-8}$, $P''(\omega)/\omega$ at $\omega \sim 0$ becomes 60% of $T=0$ limit. At the same time, $\rho_e(\omega)$ shows a small change around $\omega \sim 10^{-7}$. This means that the effect of the temperature on the conductance is rather drastic. Here we show two sorts of the magnetic excitation spectra $\chi_m''(\omega)$ and $\chi_a''(\omega)$,⁹ where $\chi_m''(\omega)$ is the imaginary part of the dynamical susceptibility of the uniform magnetic moment of local spins, $(S_{L,z} + S_{R,z})/\sqrt{2}$, and $\chi_a''(\omega)$ is that of the antiferromagnetic moment, $(S_{L,z} - S_{R,z})/\sqrt{2}$, respectively. We show the two magnetic excitation spectra at $t=0$ and $t=5.0 \times 10^{-4}$ in Fig. 7.

At $t=0$, the two spectra agree with each other. However at $t=5.0 \times 10^{-4}$, $\chi_a''(\omega)$ has the structure in lower energy region than $\chi_m''(\omega)$. It seems that $P''(\omega)$ at the main peak of the conductance is dominated by the fluctuation given by $\chi_a''(\omega)$ from Figs. 6 and 7.

We determine the two characteristic energies from $\chi_m''(\omega)$ and $\chi_a''(\omega)$ in the following ways. One is determined from the peak position of $\chi_m''(\omega)$, we call it T_M .^{20,29,31} Another one, T_{AF} , is determined as $T_{AF}/T_{AF,0} \equiv X_0/X$, where $X \equiv \lim_{\omega \rightarrow 0} \chi_a''(\omega)/\omega$.⁹ (And here we have $T_{AF,0} \equiv T_{M,0}$.) The suffix ‘‘0’’ indicates $t=0$. The quantity $T_{M,0}$ almost coincides with T_K^0 . The ratio $T_{M,0}/T_K^0$ for some cases are shown in Ref. 20.

The calculated two characteristic temperatures T_M and T_{AF} are shown in Fig. 8. They have almost same values as $t \leq 10^{-4}$. T_M monotonically increases as t increases. On the other hand T_{AF} becomes smaller near $J_{LR}^{\text{eff}} \sim T_K^0$. It has a minimum of $T_{AF} \approx 3 \times 10^{-7}$ at $t \approx 5 \times 10^{-4}$. We note that the reduction of T_{AF} near $T_K^0 \sim J$ had already been pointed out.⁸ As t increases more, T_{AF} rapidly increases. From the same analysis as for the other $\Delta/\pi U$ cases, we confirm that the minimum of T_{AF} appears for the strongly correlated cases of $\Delta/\pi U \leq 2 \times 10^{-2}$. We show T_{AF} at the main peak position in Table. II.

From the comparison with effective parameters in Fig. 3, the larger of the effective parameters $\max(t^{\text{eff}}, \Delta^{\text{eff}})$ and the smaller of the characteristic temperature $\min(T_{AF}, T_M)$ almost coincide with each other in all t , $\max(t^{\text{eff}}, \Delta^{\text{eff}}) \sim \min(T_{AF}, T_M)$.

Here we again see the temperature dependence of the conductance shown in Fig. 5 with the characteristic temperature shown in Fig. 8. We can see that T_{AF} characterizes the main peak of the conductance in finite temperature. The peak decreases as the temperature increases near $T \sim 1 \times 10^{-8}$

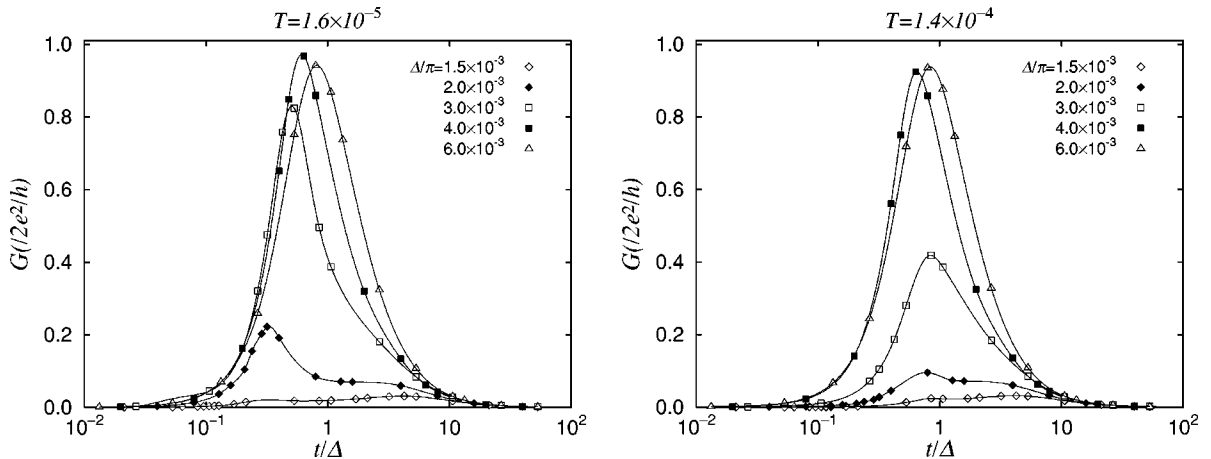


FIG. 9. Conductance from weakly to strongly correlated cases at $T = 1.6 \times 10^{-5}$ (left figure) and at $T = 1.4 \times 10^{-4}$ (right figure).

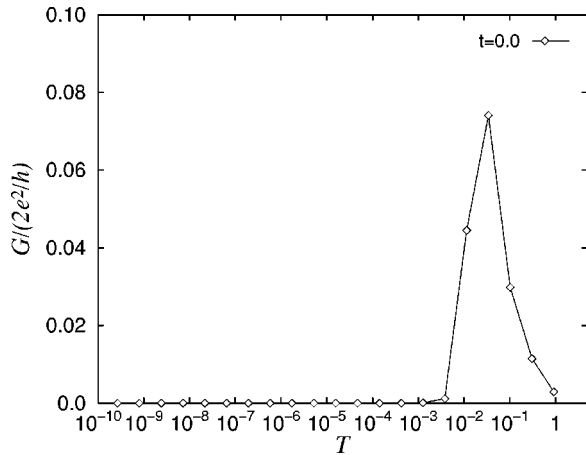


FIG. 10. Numerical results of the conductance for $t=0$ case.

$[\sim 0.1T_{\text{AF}}(t=5 \times 10^{-4})]$ in Fig. 5. As the temperature increases and reaches to $T \sim 1 \times 10^{-6}$ [$\sim 10T_{\text{AF}}(t=5 \times 10^{-4})$], the strength of the main peak becomes almost zero. Next we see the temperature dependence of the small peak. The small peak near $t \sim U/4 = 2.5 \times 10^{-2}$ increases as the temperature increases to about $T \sim 10^{-3}$ [$\sim 0.1T_{\text{M}}(t=2.5 \times 10^{-2})$]. It seems that the characteristic temperature of the conductance near the small peak is T_{M} . From above it seems that the characteristic temperature of the conductance is $\min(T_{\text{AF}}, T_{\text{M}})$ throughout the t region.

Here we show the conductance from the weakly to strongly correlated cases at fixed temperatures. We show the conductance at $T = 1.6 \times 10^{-5}$ and $T = 1.4 \times 10^{-4}$ in Fig. 9. The main peak for the strongly correlated cases is sensitive to the temperature. Then the main peak of the conductance will shift to the smaller t/Δ side with increasing peak height when the temperature decreases as seen from Fig. 9. This behavior will be observed as the split gate voltage is varied. We note that $T = 1.4 \times 10^{-4}$ corresponds to 16 mK, and $T = 1.6 \times 10^{-5}$ corresponds to 1.9 mK, for $U = 1.0$ meV systems.

Finally, we note the accuracy of the conductance calculated from Eqs. (6) and (7) by using the NRG method. It is not very accurate at very high temperatures for the small peak. In the case of $t=0$, two dots completely decouple; then the conductance should be zero. However as shown in Fig. 10, the calculated conductance has a finite value in $5 \times 10^{-3} \leq T \leq 1$ and it has a maximum at $T \sim 0.05 (= U/2)$. Thus the result at very high temperatures has ambiguities. This improper finite conductance would be caused by estimation of Eq. (6) at $\omega \sim T$ instead of $\omega \rightarrow 0$. The finite value in the current spectrum at $T \sim 0.05$ would reflect the largeness of the dynamical charge fluctuation in the dots.

IV. SUMMARY AND DISCUSSION

We calculated the tunneling conductance through the two quantum dots that connected to the left lead and the right lead in series. We investigated the effect of the kinetic exchange coupling between the dots, and also the competition with the Kondo effect.

As the hopping between the two dots increased, (i) Kondo singlet state of each dot with its adjacent-site lead, (ii) local singlet state, and (iii) molecular orbital like state with double occupancy in even state, continuously appeared. The crossover occurred between (i) and (ii), (ii) and (iii), each other. For $t \ll U$ cases, the Kondo binding between the left (right) lead and the left (right) dot T_{K}^0 and the antiferromagnetic kinetic exchange coupling between the two dots $J_{\text{LR}}^{\text{eff}}$ competed. The boundary between (i) and (ii) was characterized as $J_{\text{LR}}^{\text{eff}} \sim T_{\text{K}}^0$, where we have the relation $t^{\text{eff}} \sim \Delta^{\text{eff}}$, and the tunneling conductance showed a peak. This peak had the unitarity limit value of $2e^2/h$ reflecting the coherent connection through the lead-dot-dot-lead. At $t \sim U/4$ of the boundary between (ii) and (iii), we had a small peak.

The system showed the strongly correlated behaviors for $\Delta/\pi U \leq 2 \times 10^{-2}$ ($u \equiv U/\pi\Delta \geq 5$) cases. The borders of (i)-(ii) ($J_{\text{LR}}^{\text{eff}} \sim T_{\text{K}}^0$) and (ii)-(iii) ($t \sim U/4$) were clearly distinguished, then there were the two peak structures in the conductance. Furthermore the width of the main peak became steeply narrow. The characteristic temperature of the main peak was strongly reduced compared with the Kondo temperature of the single dot systems T_{K}^0 . These anomalous behaviors of the main peak related to the quantum critical transition of the two-impurity Kondo problem studied previously. Though the hopping term had conflicting effects on the critical transition of the two-impurity Kondo systems, generation of it through the kinetic exchange coupling and suppression of it due to the parity splitting, we found that we see the sign of the anomaly in the tunneling conductance.

The quantitative calculation shown in this paper gave the new realization for the two-impurity Kondo problem. This investigation suggested the importance of the systematic study of the DQD systems for the two-impurity Kondo problem.

ACKNOWLEDGMENTS

This work was partly supported by a Grant-in-Aid for Scientific Research on the Priority Area ‘‘Spin Controlled Semiconductor Nanostructures’’ (Grant No. 11125201) from the Ministry of Education, Science, Sports and Culture, Japan. The numerical computation was partly performed at the Supercomputer Center of Institute for Solid State (University of Tokyo), the Computer Center of Institute for Molecular Science (Okazaki National Research Institute), and the Computer Center of Tohoku University. One of the authors (W.I.) was supported by the JSPS.

*Email address: izumida@tarucha.jst.go.jp

¹A. C. Hewson, *The Kondo Problem to Heavy Fermions* (Cambridge University Press, Cambridge, UK, 1993).

²K. Yosida, *Theory of Magnetism* (Springer, New York, 1996).

³B. A. Jones, C. M. Varma, and J. W. Wilkins, Phys. Rev. Lett. **58**, 843 (1987).

⁴B. A. Jones, C. M. Varma, and J. W. Wilkins, Phys. Rev. Lett. **61**, 125 (1988).

⁵B. A. Jones and C. M. Varma, Phys. Rev. B **40**, 324 (1989).

⁶B. A. Jones, Physica B **171**, 53 (1991).

⁷B. A. Jones, B. G. Kotlar, and A. J. Mills, Phys. Rev. B **39**, 3415 (1989).

⁸O. Sakai, Y. Shimizu, and T. Kasuya, Solid State Commun. **75**, 81 (1990).

⁹O. Sakai and Y. Shimizu, J. Phys. Soc. Jpn. **61**, 2333 (1992); **61**, 2348 (1992).

- ¹⁰R. M. Fye, J. E. Hirsch, and D. J. Scalapino, *Phys. Rev. B* **35**, 4901 (1987).
- ¹¹R. M. Fye and J. E. Hirsch, *Phys. Rev. B* **40**, 4780 (1989).
- ¹²R. M. Fye, *Phys. Rev. Lett.* **72**, 916 (1994).
- ¹³I. Affleck and A. W. W. Ludwig, *Phys. Rev. Lett.* **68**, 1046 (1992).
- ¹⁴I. Affleck, A. W. W. Ludwig, and B. A. Jones, *Phys. Rev. B* **52**, 9528 (1995).
- ¹⁵D. Goldhaber-Gordon, H. Shtrikman, D. Mahalu, D. Abusch-Magder, U. Meirav, and M. A. Kastner, *Nature (London)* **391**, 156 (1998).
- ¹⁶S. M. Cronenwett, T. H. Oosterkamp, and L. P. Kouwenhoven, *Science* **281**, 540 (1998).
- ¹⁷D. Goldhaber-Gordon, J. Göres, M. A. Kastner, H. Shtrikman, D. Mahalu, and U. Meirav, *Phys. Rev. Lett.* **81**, 5225 (1998).
- ¹⁸J. Schmid, J. Weis, K. Eberl, and K. Klitzing, *Physica B* **256-258**, 182 (1998).
- ¹⁹F. Simmel, R. H. Blick, J. P. Kotthaus, W. Wegscheider, and M. Bichler, *Phys. Rev. Lett.* **83**, 804 (1999).
- ²⁰O. Sakai, W. Izumida, and S. Suzuki, *Proceedings of the Fourth International Symposium on Advanced Physical Field, Tsukuba, Japan, 1999* (National Research Institute for Metals, Tsukuba, 1999), p. 143; W. Izumida and O. Sakai, *Physica B* **281-282**, 32 (2000); W. Izumida, O. Sakai, and S. Suzuki (unpublished).
- ²¹For an example of the recent experimental studies of the double dot systems, T. H. Oosterkamp, T. Fujisawa, W. G. van der Wiel, K. Ishibashi, R. V. Hijman, S. Tarucha, and L. P. Kouwenhoven, *Nature (London)* **395**, 873 (1998); T. Fujisawa, T. H. Oosterkamp, W. G. van der Wiel, B. W. Broer, R. Aguado, S. Tarucha, and L. P. Kouwenhoven, *Science* **282**, 932 (1998).
- ²²T. Ivanov, *Europhys. Lett.* **40**, 183 (1997).
- ²³T. Pohjola, J. König, M. M. Salomaa, J. Schmid, H. Schoeller, and Gerd. Schön, *Europhys. Lett.* **40**, 189 (1997).
- ²⁴T. Aono, M. Eto, and K. Kawamura, *J. Phys. Soc. Jpn.* **67**, 1860 (1998).
- ²⁵W. Izumida, O. Sakai, and Y. Shimizu, *Physica B* **259-261**, 215 (1999).
- ²⁶A. Georges and Y. Meir, *Phys. Rev. Lett.* **82**, 3508 (1999).
- ²⁷N. Andrei, G. T. Zimányi, and G. Schön, *Phys. Rev. B* **60**, 5125 (1999).
- ²⁸W. Izumida and O. Sakai, *Physica B* **284-288**, 1764 (2000).
- ²⁹W. Izumida, O. Sakai, and Y. Shimizu, *J. Phys. Soc. Jpn.* **67**, 2444 (1998).
- ³⁰We have neglected the energy and parity dependence of the hybridization matrix. Usually it suppresses the occurrence of the artificial quantum critical transition of the two-impurity Kondo problem. It is essentially important to take into account a mechanism, which causes the parity splitting of the electron occupation number to obtain a correct answer for this problem. In the present calculation, the parity splitting is caused by the hopping term. We think that the present hopping term should be considered as an effective one including the indirect part caused by the energy and parity dependence of the hybridization matrix.
- ³¹W. Izumida, O. Sakai, and Y. Shimizu, *J. Phys. Soc. Jpn.* **66**, 717 (1997).